

## 3D Point Clouds Extraction from High-Resolution Multi-View Satellite Images Using Dense Image Matching

Won-Suk Kwon(1), Mi-Kyeong Kim(1), Young-Rim Lee(1),

Hyeon-Seung Song(1), Dae-Sik Shin(1)

<sup>1</sup> Agency of Defense Development, Yuseong P.O. Box 35, Yuseong-gu, Daejeon, Korea

Email: [wskwon@add.re.kr](mailto:wskwon@add.re.kr), [mikyeong@add.re.kr](mailto:mikyeong@add.re.kr), [yrlee@add.re.kr](mailto:yrlee@add.re.kr), [hssong@add.re.kr](mailto:hssong@add.re.kr),  
[ds shin@add.re.kr](mailto:ds shin@add.re.kr)

**KEY WORDS:** RPC, multi-view, SGM, point cloud, DSM

**ABSTRACT:** It is possible to generate precise digital surface models (DSMs) by applying image matching techniques to high-resolution stereo satellite images. Recently, Semi-global matching (SGM) is widely used for DEM generation from stereo satellite images and its stable performance has been proved through previous studies. This paper aims to extract 3D point clouds from multi-view satellite images that include stereo images and mono images using SGM. In the first stage of the point cloud extraction, the rational polynomial coefficient (RPC) bias errors are corrected by using RPC block adjustment model. After searching the optimal stereo image pair, epipolar images are generated with updated RPCs. Then, SGM algorithm is applied to the epipolar images for extracting a point cloud. In the matching process, the matching cost is calculated by using census transform and 8-path aggregation and the disparity map resulting from SGM is generated. Using the disparity map derived from SGM, the tie points in a pair of images are extracted. It is possible to determine three-dimensional position of the tie points, resulting in the 3D point cloud for generating a precise DEM.

## 1. INTRODUCTION

With the development of image matching techniques, it is possible to generate precise and accurate digital surface models (DSMs) using high-resolution satellite images. Recently, many researchers have been studying the generation of high-resolution point clouds and DSMs using drone images. The drone can acquire lots of images with high overlap rate and it enables point clouds generation by structure from motion (SfM) technique. However, in the case of the inaccessible area, DSM is generally generated using satellite images. Since it is difficult to acquire a large number of images from satellites unlike drones, point clouds from satellite images are generated through the dense image matching. Among many studies related to dense image matching, Hirschmuller (2008) proposed the semi-global matching (SGM) technique. SGM is widely used for DSM generation and its performance has been verified through previous studies and commercial software for photogrammetry. The purpose of this study is to generate 3D point clouds from multi-view satellite images using SGM technique, and compare the quality of generated point clouds according to geometry conditions of satellite image pair.

## 2. MULTI-VIEW SATELLITE IMAGES

### 2.1 METHOD

In order to extract 3D point clouds using multi-view satellite images, RPC block modeling is performed using ground control points (GCPs) and RPC bias errors are corrected(Choi, 2012). Then, epipolar images are generated by analyzing epipolar geometry of all images. The 3D point clouds are extracted after dense image matching between each generated epipolar image pair(Rongjun, 2017). After performing SGM between each generated epipolar images pair, the 3D point clouds can be extracted from matching results. Overall process is described in Figure 1.

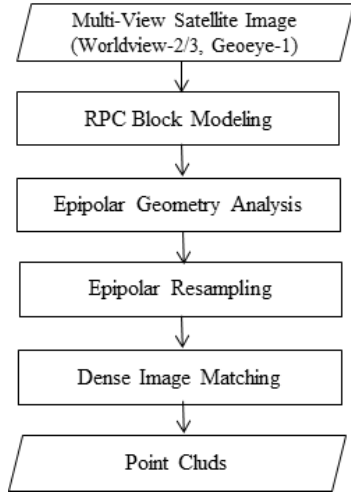


Figure 1. Workflow for Point Cloud generation



Figure 2. Footprint and GCPs of Multi-view satellite images

## 2.2. TEST DATASET

Test dataset have different dates as shown in Table 1. Worldview-2 images used in this study were stereo pair with ortho-ready standard stereo product, and the other images were mono images with ortho-ready standard product. The distribution of GCPs in the study area is shown Figure 2. The RPC block modeling results have shown that longitude RMSE was 0.359m, latitude RMSE was 0.126m, height RMSE was 0.257m.

Table 1. Test Dataset Properties

Image ID	Platform Type	Date	Resolution	Product
WV2-01	WorldView-2	2017-06-15	40cm	Ortho Ready Standard Stereo
WV2-02	WorldView-2	2017-06-15	40cm	Ortho Ready Standard Stereo
GE1-01	GeoEye -1	2014-02-24	40cm	Ortho Ready Standard
GE1-02	GeoEye-1	2014-11-10	40cm	Ortho Ready Standard
WV2-03	WorldView-2	2018-02-20	40cm	Ortho Ready Standard
WV3-01	WorldView-3	2015-03-22	40cm	Ortho Ready Standard

## 2.3 GENERATION OF EPIPOLAR IMAGE

Total of 15 pairs of epipolar image pairs were generated from 6 scenes of multi-view satellite images using unified piecewise epipolar resampling method developed by Koh and Yang (2016). The optimal epipolar geometry was known as convergence angle (CA)  $30^{\circ}$ - $60^{\circ}$ , and the stereoscopic pairs WV2-01 and WV2-02 epipolar geometry have  $33^{\circ}$  CA,  $60.2^{\circ}$  bisector angle (BA), and  $6.7^{\circ}$  asymmetry angle (AA). Besides stereo pair, epipolar images were generated using the combination of every single image, and have a various range of convergence angle from 10 to  $57.6$  degrees.

## 3. POINT CLOUDS GENERATION USING MULTI-VIEW SATELLITE IMAGES

### 3.1 SEMI-GLOBAL MATCHING

We used SGM for image matching for clipped each epipolar image ( $1200 \times 1200$  pixel) in the test site. SGM proceeds through cost calculation, cost aggregation, and disparity computation. In this paper, we used Census Transform for cost calculation, and applied to 8 directions of cost aggregation using Equation (1). It was used  $7 \times 7$  window for Census Transform, the penalty parameters used in the study were  $P1 = 15$ ,  $P2 = 90$  (d'Angelo, 2011,

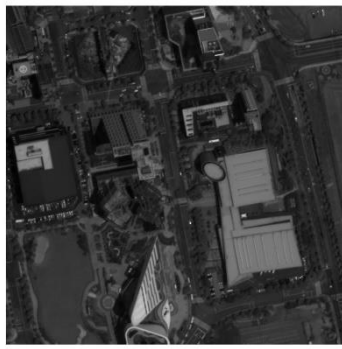
Wonsuk,2018).

The disparity was computed for each pixel using Aggregated COST in equation (1) then the disparity map was generated.

$$L_r = C(p, d) + \min(L_r(p-r, d), L_r(p-r, d-1) + P_1, L_r(p-r, d+1) + P_1, \min_i L_r(p-r, i) + P_2) - \min_k L_r(p-r, k) \quad (1)$$

### 3.2 POINT CLOUD

We generated 15 point clouds through image matching. Figure 3 and Figure 4 shows the point clouds from optimal and poor epipolar geometry conditions among homogeneous sensor type. The epipolar geometry in Figure 3 has good geometry from stereo pair image, and the generated point cloud has high quality. Meanwhile, the point cloud in Figure 4 shows a lot of noises because of poor epipolar geometry condition among homogeneous sensors and the loss of points due to mismatching. However, the point cloud in Figure 5 shows the points on the facade of the building because images were acquired from similar geometry.



(a) WV2-01-Epipolar Image

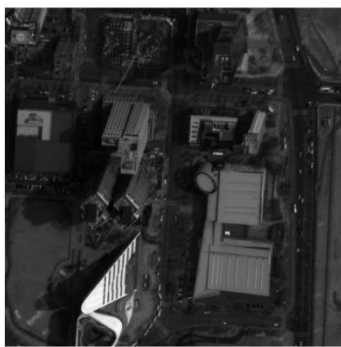


(b) WV2-02-Epipolar Image



(c) Point Cloud

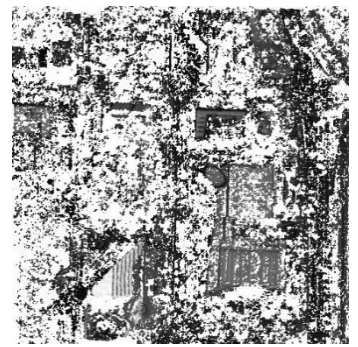
Figure 3. WV2-01/ WV2-02 epipolar pair (C.A 33 A.A 6.7 BIE 60.2 B/H 0.6) and Point cloud



(a) WV2-01-Epipolar Image



(b) WV2-03-Epipolar Image



(c) Point Cloud

Figure 4. WV2-01/ WV2-03 Epipolar pair (C.A 12.7 A.A 3.8 BIE 59.3 B/H 0.26) and Point cloud

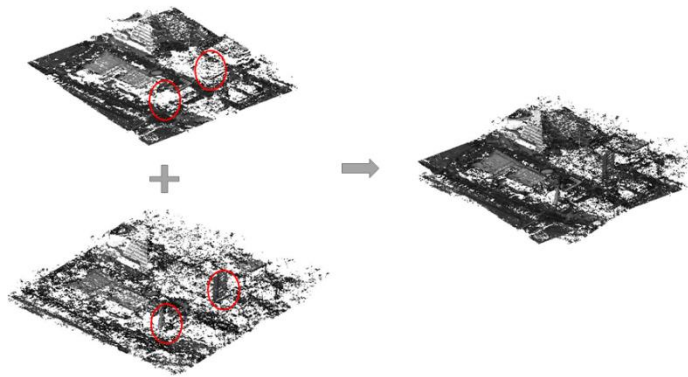


Figure 5. Overlay with WV2-01/WV-02 and WV2-01/WV2-03

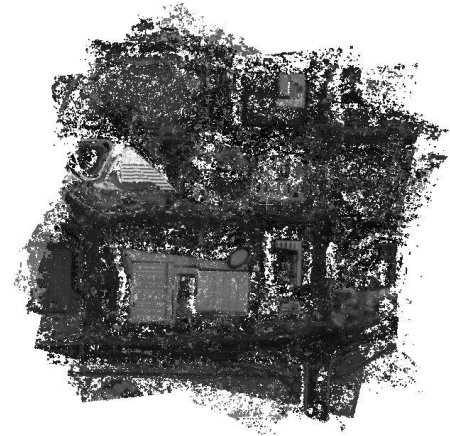


Figure 6. Overlay with 6-pairs

## 4. CONCLUSION

In this study, we generated 15 pairs of epipolar images from different geometry condition using 6 scenes from multi-view satellite images and compared the quality of generated point clouds through SGM.

We confirmed that stereo pair that has convergence angle below 30 degrees showed generally poor matching quality. Although the epipolar geometry has poor condition, we confirmed the possibility of points extraction on the facade of the building. At the beginning of this study, we expected that point cloud registration from a number of pairs can generate a high-quality point clouds or DSM compared to using a pair of stereo images. The results of this study showed unsatisfactory point cloud quality because the point cloud has noise and large height errors. To overcome the shortcomings, we will study about noise removal and point cloud matching for further research.

## References

- Choi, S.Y. and Kang, J.M., 2012. Accuracy Investigation of RPC-based Block Adjustment Using High Resolution Satellite Images GeoEye-1 and WorldView-2. *Journal of the Korean Society of Surveying, Geodesy, Photogrammetry and Cartography*, 30(2): 107-116
- d'Angelo, P. and Reinartz, P., 2011. Semiglobal matching results on the isprs stereo matching benchmark. In: *ISPRS Hannover Workshop 2011: High-Resolution Earth Imaging for Geospatial Information*.
- Gabriele, F., Carlo de F., and Enric M., 2017. Automatic 3D Reconstruction from Multi-Date Satellite Images, *CVPR*
- Hirschmuller, H., 2008. Stereo Processing by Semiglobal Matching and Mutual Information, *IEEE Transactions on Pattern Analysis and Machine Intelligence*, 30(2), pp.328-341
- Koh., J.W. and Yang., H.S., 2016, Unified piecewise epipolar resampling method for pushbroom satellite images. *EURASIP Journal on Image and Video Processing*.
- Rongjun, Q. 2017. Automated 3D recovery from high resolution multi-view satellite images, *ASPRS 2017 Annual Conference*
- Wonsuk, K., 2019. DSM Generation and Accuracy Comparison Using Stereo Matching Based on Images Segmentation., *Korean Journal of Remote Sensing*, 35(3), pp.401-413